This is an *Accepted Manuscript*, which has been through the RSC Publishing peer review process and has been accepted for publication.

Accepted Manuscripts are published online shortly after acceptance, which is prior to technical editing, formatting and proof reading. This free service from RSC Publishing allows authors to make their results available to the community, in citable form, before publication of the edited article. This *Accepted Manuscript* will be replaced by the edited and formatted *Advance Article* as soon as this is available.

To cite this manuscript please use its permanent Digital Object Identifier (DOI®), which is identical for all formats of publication.

More information about *Accepted Manuscripts* can be found in the **Information for Authors**.

Please note that technical editing may introduce minor changes to the text and/or graphics contained in the manuscript submitted by the author(s) which may alter content, and that the standard **Terms & Conditions** and the **ethical guidelines** that apply to the journal are still applicable. In no event shall the RSC be held responsible for any errors or omissions in these *Accepted Manuscript* manuscripts or any consequences arising from the use of any information contained in them.

Nanoscale

Nanoparticle Dispersion in Polymer Nanocomposites by Spin-Diffusion-Averaged Paramagnetic Enhanced NMR Relaxometry

Bo Xu,[a]* Johannes E. Leisen,[b] and Haskell W. Beckham [a]

We developed an analytical relationship between nuclear magnetic relaxation and interparticle spacings in polymer nanocomposites filled with paramagnetic-impurity-containing clay nanoparticles. Using ^{1}H NMR relaxometry, clay nanoparticle dispersion was quantified and agrees with interparticle spacing distributions determined from statistical analysis of TEM images. Some information on the overall quality of clay dispersion is revealed. This work offers a new approach and new insights into nanoparticle dispersion in polymer nanocomposites.

Incorporation of nanoparticles into polymers produces high performance nanocomposites in which properties are governed by filler dispersion, surface chemistry and morphology.[1-8] Considerable efforts have been devoted to relating their ultimate properties with nanoparticle dispersion. The interparticle spacing (IPS), a measure of the size of unfilled polymer between particles, has been correlated with macroscale performance in experiments and computer simulations.[6-15] Despite some advances, quantitative characterization of the interparticle spacing in bulk materials is challenging and time-consuming, and yet important for the advancement of composite nanotechnology.

Polymer-clay nanocomposites (PCNs), an important class of organic-inorganic layered nanomaterial,[3] have been applied in large quantities.[16, 17] The interparticle spacing is governed by the chemical and physical properties of the starting clay material, the loading and the processing details. The resulting clay particle structures are described as exfoliated, intercalated or tactoid. Often, a mixture of these structures is observed in the same material,[5, 18] which leads to difficulties in quantifying and describing the interparticle spacing. Currently, despite its time requirements, transmission electron microscopy (TEM) is the most commonly used tool to evaluate IPS. From TEM images, IPS can be estimated by various semi-quantitative statistical methods, such as the free-path spacing measurement.[19, 20]

Solid-state nuclear magnetic resonance (NMR) methods have been employed to determine clay exfoliation levels and homogeneity of clay distribution in PCNs, but require additional TEM and X-ray diffraction (XRD) data on the same samples.[21-27] The NMR methods take advantage of the effect of paramagnetic impurities in natural clay on the ^{1}H spin-lattice relaxation times (T_1^H). The T_1 relaxation times of the polymer matrix in PCNs are largely reduced by dispersed clay minerals such as montmorillonite (MMT). These clays often contain paramagnetic Fe^{3+} ions (typically, $0.1 \sim 5$ wt% as Fe_2O_3), which are substituted at Al^{3+} sites within central alumina layers sandwiched between two silica layers. Note that the three-layer 'sandwich' constitutes a single 1-nm-thick platelet.[28] The Fe^{3+} ions shorten the T_1^H of the polymer matrix in two ways: via direct interaction with neighboring nuclei, and via spin diffusion from remote nuclei.[21-27] In rigid PCNs containing these clays, ^{1}H spin diffusion spreads the paramagnetic-enhanced relaxation throughout the whole sample, which provides a mechanism to probe distances between clay nanoparticles. This is exactly the information needed for these materials whose bulk physical properties are governed by the distribution of clay nanoparticles.

Recent studies on PCNs have reported qualitative correlations of NMR-measured T_1^H with TEM-measured IPS. Computer simulations suggest that the T_1^H relaxation rate is a function of the IPS.[26, 27] However, this correlation has not been analytically described or verified; the pioneering NMR studies depended on information determined with TEM and/or XRD methods. Here, we report an analytical relation between the NMR T_1 relaxation and the IPS, and then use it to measure interparticle spacings in bulk polymer nanocomposites. We then quantitatively compare our NMR results with TEM data. By doing so, this work offers a better understanding of the structural quantification of PCNs by NMR relaxometry.

To connect NMR T_1 relaxation data with the IPS, we first focus on mathematically describing NMR magnetization growth collected by saturation-recovery experiments. Magnetization growth occurs due to relaxation recovery following a train of saturation pulses. To compute the NMR T_1 relaxation, we begin with a simple one-dimensional (1D) lamellar model (Fig. 1a). The paramagnetic-impurity-containing clay particles and their surface layers act as relaxation sinks. The number of nuclei in the surface layers are much less than those in the bulk of the polymer matrix at low clay loadings (*e.g.*, < 5 wt%); these nuclei mainly contribute to a fast initial relaxation recovery due to direct electron-nucleus interactions.[21] Here, the focus of our model is on the magnetization growth that

arises from the more numerous bulk nuclei in the regions between relaxation sinks.

Consequently, our model is characterized by four main parameters: the characteristic relaxation time, $T_{1,s}$ of relaxation sinks, the relaxation time, $T_{1,m}$ of the polymer matrix, the average spin diffusion coefficient of the polymer matrix, D, and the interparticle spacing, Δ (Fig. 1a). Regardless of the details of the relaxation by direct interaction, the relaxation of surface nuclei should approach the equilibrium magnetization asymptotically, despite the spatial dependence. As such, we semi-empirically assume that surface nuclei exhibit a characteristic relaxation time, $T_{1,s}$,[27] which can be described by the time-dependent magnetization in saturation-recovery experiments: $m_s(t) = m_0[1 - \exp(- t/T_{1,s})]$, where m_0 is the equilibrium magnetization per nucleus. This assumption allows our model to include infinitely fast relaxation as a special case, that is, the sinks are always maintained at thermal equilibrium, $m_s(t) = m_0$).[29, 30] Thus, $m_s(t) \rightarrow m_0$, as $T_{1,s} \rightarrow 0$.

Furthermore, the thickness of the surface layer, b (e.g., ~ 0.4 nm reported previously[25-27]) is assumed to be much less than the average of the IPS, $\langle\Delta\rangle$, so that $\langle\Delta\rangle \approx 2L$, where $2L$ is the distance between sinks (Fig. 1a). Typical PCNs fulfill this assumption nicely, e.g., $\langle\Delta\rangle$ is ~ 50 nm for 5 wt% MMT-filled PCNs that exhibit an idealized repeating lamellar structure of alternating polymer and clay.[5, 18] For less than ideal dispersion, the inequality holds; $b << \langle\Delta\rangle$, as $\langle\Delta\rangle$ becomes large.
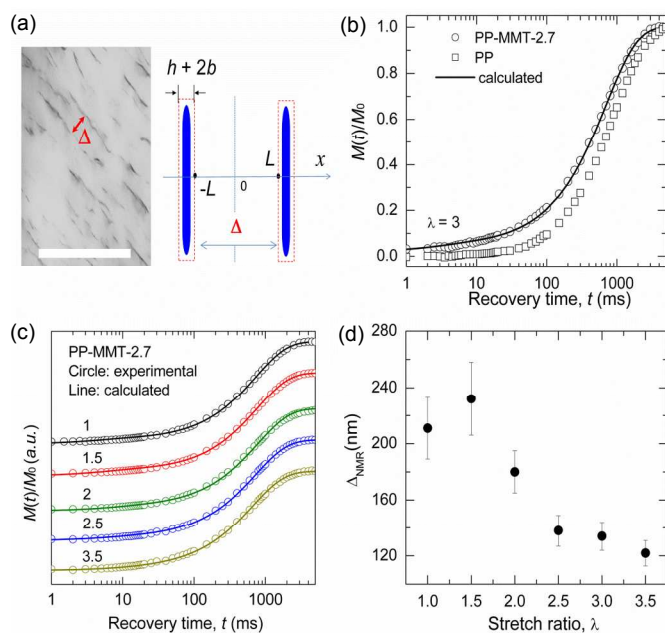
Fig. 1 (a) Representative TEM image (left) of a nanocomposite of polypropylene (PP) and 2.7 wt% montmorillonite (MMT), PP-MMT-2.7, after equi-biaxial stretching to a final length/initial length ratio (λ) of 3 (the white scale bar is 500 nm). One-dimensional lamellar model (right) showing the interparticle spacing, Δ, between h-thick clay particles with b-thick surface layers that act as relaxation sinks. (b,c) Normalized ^{1}H NMR signal intensity (i.e., magnetization) as a function of recovery time, t, for PP–MMT–2.7 films (λ shown above the data), on which the solid lines are the best fits to Eq. 1. The NMR relaxation profile of a representative unfilled PP film with $\lambda = 3$ is shown in (b). The profiles in (c) are vertically shifted to avoid overlap. (d) The resulting Δ as a function of stretch ratio.

Based on the above model, an analytical description of the detected NMR signal intensity is given as the normalized magnetization, $M(t)/M_0$, of the unfilled domain (see ESI Section 3 for specific details[†]):

$$\frac{M(t)}{M_o} = 1 - \left(\frac{4D}{\beta\Delta^2}\right)^{1/2} \tan\left(\frac{\beta\Delta^2}{4D}\right)^{1/2} \exp(-t/T_{1,s})$$
$$- \frac{8}{\pi^2}\sum_{n=0}^{\infty}\frac{1}{(2n+1)^2}\left[\frac{1}{1-(2n+1)^2\pi^2D/(\beta\Delta^2)}\right]\exp\left[-\left(\frac{(2n+1)^2\pi^2D}{\Delta^2}+\frac{1}{T_{1,m}}\right)t\right]$$

(1)

where M_0 is the total equilibrium magnetization, D is the bulk spin diffusion coefficient (uniform, not a function of spatial position), $1/T_{1,m}$ is the bulk matrix nuclear relaxation rate, and β is the difference between relaxation rates of the surface nuclei and the bulk matrix nuclei, which is given by $\beta = 1/T_{1,s} - 1/T_{1,m}$.

The relaxation efficiency of the sinks is reflected by $1/T_{1,s}$, or more accurately by β; that is, the shorter the $T_{1,s}$ (or larger the β), the higher the efficiency. Analysis of our model reveals that magnetization growth critically depends on $T_{1,s}$ at initial recovery times (see ESI Fig. S2[†]). The overall relaxation is weakly related to $T_{1,s}$ if the sink relaxation is sufficiently efficient, but is significantly delayed if the sink relaxation rate is inadequate, for example, when $T_{1,s} > 10$ ms. Thus, it is important to understand the relaxation efficiency of surface nuclei when using this model to analyze different types of PCNs. Estimates of $T_{1,s}$ can be obtained from relaxation times of nuclei on clay surfaces.[21, 25, 26] The $T_{1,s}$ of surface nuclei strongly depends on the concentration of paramagnetic ions due to the direct electron-nucleus interaction.[24, 26] Surface nuclei in widely studied MMTs (e.g., from Southern Clay Products, typically containing ~5 wt% Fe_2O_3) exhibit $T_{1,s}$ on the order of a few milliseconds at magnetic fields up to several hundred MHz.[25-27]

To demonstrate the approach, a series of polypropylene–montmorillonite (PP–MMT) nanocomposite films with six stretch ratios (λ = final length/initial length) were characterized by ^{1}H NMR relaxometry and TEM (see ESI Experimental Detail[†]). The Fe percentage of the neat MMT was calculated to be 4.96 wt% Fe_2O_3; the T_1^H of the neat organically modified MMT is 10 ms, which was measured at a magnetic field of 7.05 Tesla.[25] The ^{1}H NMR data reveal that the PP–MMT samples exhibit faster magnetization growth than the neat PP (cf. Fig. 1b), illustrative of the paramagnetic enhancement on T_1^H. Magnetization growth profiles of the nanocomposites (cf. Figs 1b,c) were fitted to Eq. 1 using the following parameters: $D = 0.24$ nm^2/ms, $T_{1,m} = 810$, 849, 885, 860, 820 and 805 ms for the corresponding neat PP films with $\lambda = 1$ up to 3.5, respectively. The $T_{1,m}$ values were determined by fitting relaxation profiles of the neat PP to an exponential function. The initial fitting values of Δ and $T_{1,s}$ should be reasonably estimated, whereas the values of D and $T_{1,m}$ for the nanocomposites should be experimentally determined (see ESI Section 5[†]). For instance, an appropriate initial value for Δ is an idealized spacing for full exfoliation;[5] $T_{1,s}$ can be estimated from relaxation times of nuclei in the neat organically modified clay. Here, we used D and T_1^H of the PP to fit the profile of the corresponding PP–MMT, as the unfilled and filled samples show almost identical crystallinity for a given stretch ratio.[25] Spin-diffusion coefficients, D have been reported for many polymers.[31, 32] Here we used a known D to determine Δ. Conversely, one could also use this method to determine D on samples for which Δ is known.

As seen in Figures 1b and 1c, we obtained excellent fits in the long-time regime and fairly good fits in the short-time regime. Interparticle spacings were determined from the best fits and are shown in Figure 1d as a function of stretch ratio. Beginning with $\lambda = 1.5$, the NMR-derived interparticle spacings decrease upon stretching. The fact that the unstretched PP-MMT sample, $\lambda = 1$,

does not follow this pattern is not a deficiency of the model, but rather arises from the details in the spatial distribution of MMT particles upon stretching and will be discussed below. Hence, an important question arises as to how the NMR-derived interparticle spacings are related to clay dispersion with respect to the average IPS and the spacing distribution. Thus, we quantitatively compared these NMR results with TEM images that directly reveal the spatial distribution of MMT particle spacings.

We measured the distribution of interparticle spacings from TEM images for each sample, as shown in Figure 2 for representative examples. The alignment, size and aspect ratio of particles vary upon stretching (cf. Fig. 2a,b).[25] The distance between particles was determined for each sample from TEM images using the free-path spacing measurement (FPSM) method modified to ignore the distance between platelets inside particles (see ESI Methods[†] and Fig. S1[†]). This modification allows a direct comparison between the TEM and NMR results because the latter analysis only deals with the bulk matrix between clay particles. From the TEM analysis, the probability density and cumulative distributions of interparticle spacings were constructed (cf. Fig. 2c,d). These results show that the IPS distribution remains asymmetric but shifts to smaller spacings and becomes narrower with increasing stretch ratio. Both Gaussian and log-normal functions provide fair fits to the spacing distribution in the unstretched sample ($\lambda = 1$). For the higher stretch ratios, the log-normal is a superior fit to the Gaussian distribution. Such a positively skewed distribution has been observed often in PCNs.[19, 20] Most spacings appear at the lower end of the distribution, while smaller numbers of spacings occur toward the upper end. Fig. 2d reveals that interparticle spacings are largely reduced by a stretch ratio of 2.5, above which only slight decreases occur.
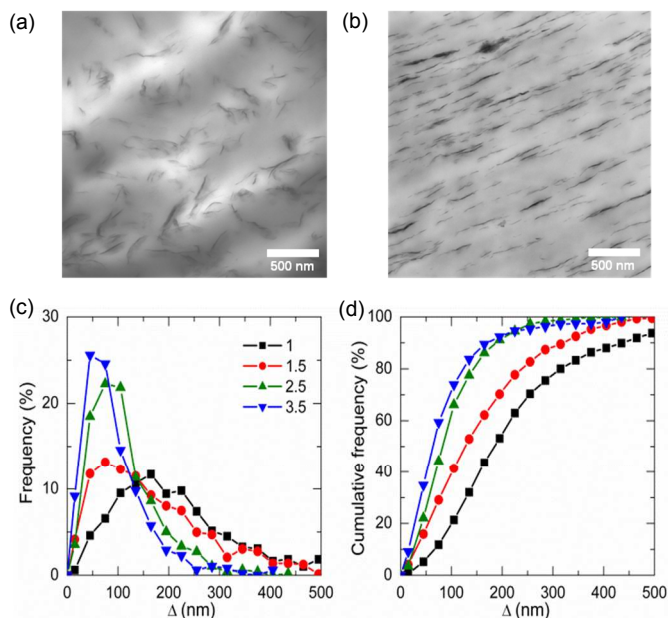
Fig. 2 Representative TEM images of a nanocomposite of polypropylene (PP) and 2.7 wt% montmorillonite (MMT), PP-MMT-2.7, after equi-biaxial stretching to a final length/initial length ratio (λ) of 1(a) and 3.5 (b). Distribution of interparticle spacings, Δ (c) and the corresponding cumulative distribution (d) for stretch ratios of 1, 1.5, 2.5 and 3.5 determined from the TEM images.

Figure 3a compares the interparticle spacings derived from the NMR and TEM analyses for the PP–MMT–2.7 samples. Data are shown for the NMR IPS (Δ_{NMR}), the TEM arithmetic average IPS (Δ_{TEM_ave}) and the TEM root-mean-square average (Δ_{TEM_rms}) versus

the TEM root-mean-square average IPS. The most commonly held view is that the NMR analysis provides the arithmetic average IPS, which has been normally verified by small-angle X-ray scattering or TEM.[31, 32] However, we find that the Δ_{NMR} values are larger than the Δ_{TEM_ave} values, except for the unstretched sample in which the Δ_{NMR} is identical to the Δ_{TEM_ave}. For the stretched samples, a much better correlation is found between Δ_{NMR} and Δ_{TEM_rms}, reflecting the change in the IPS distribution that occurs upon stretching (cf. Fig. 2c).

These results raise the question of how Δ_{NMR} is related to the IPS distribution. According to Eq. 1, the magnetization growth is a function of Δ^2. Since there are numerous interparticle spacings in technical PCNs, the relaxation profiles should be described by a function of the distribution of Δ^2. We note that fitting the data to Eq. 1 using either Δ^2 or Δ provides a consistent value for Δ_{NMR}. It therefore follows that the resultant Δ_{NMR} should be associated quantitatively with the root-mean-square or quadratic mean (Δ_{TEM_rms}) of the IPS distribution. When compared with the IPS arithmetic average, the quadratic mean ensures that the large spacings at the upper end of the positively skewed distribution are weighted more heavily than the small spacings in regard to their contribution to the magnetization growth. The large spacings play a more dominant role in the magnetization growth in the long-time regime (see ESI Fig. S3[†]). For a log-normal distribution, Δ_{TEM_rms} should be more comparable to Δ_{NMR} than Δ_{TEM_ave}, which is confirmed in Figure 3a for the stretched samples.
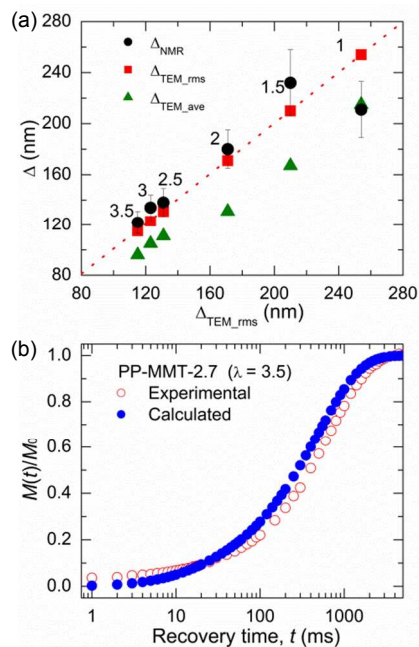
Fig. 3 (a) Comparison between the NMR-derived (circles, Δ_{NMR}) and TEM-measured interparticle spacings in PP-MMT nanocomposite films (stretch ratios shown above the data): the TEM arithmetic average (triangles, Δ_{TEM_ave}) and the TEM quadratic mean (squares, Δ_{TEM_rms}) (see ESI Table S1[†] for more details). (b) Magnetization growth profiles for the PP–MMT–2.7 sample with $\lambda = 3.5$. The calculated profile was created using the TEM IPS distribution shown in Fig. 2c, Eq. 1, and the same parameters used and determined from fitting the NMR experimental profile, which is the same as that shown in Fig 1c ($D = 0.24$ nm^2/ms, $T_{1,m} = 806$ ms, $T_{1,s} = 6.1$ ms).

Despite the general consistency of the NMR and TEM results, the Δ_{NMR} values are slightly larger than the Δ_{TEM_rms} values for all of the stretched samples (cf. Fig 3a). This is attributed to the possibility that the spatial distribution of MMT particles is non-uniform in these

PP–MMT–2.7 nanocomposites. To examine the effect of the IPS distribution on the NMR relaxation data, we calculated a magnetization growth profile for the PP–MMT–2.7 sample with $\lambda = 3.5$ using the TEM-determined IPS distribution shown in Fig. 2c, Eq. 1, and the same parameters used and determined from fitting the NMR experimental data shown in Fig. 1c. This calculated magnetization growth profile is shown in Fig. 3b as the solid circles. The NMR experimental magnetization growth profile is shown in Fig. 3b as the open circles. The NMR experimental profile exhibits faster recovery in the short-time regime, but slower recovery in the long-time regime. Detailed analyses using the model (see ESI Fig. S3[†]) have shown that this behavior is consistent with broader distributions of the IPS. Thus, the NMR data are indicating a broader IPS distribution than the TEM data for the stretched samples. TEM measurements are made on tiny two-dimensional pieces of microtomed samples and may not be representative of the bulk material.[33] NMR measurements are averaged over a much larger portion of the sample, and therefore reflect a more global average. The asymmetric shape of the IPS distribution, in which the larger fraction exhibits smaller IPS values, dictates that TEM snapshots of localized regions will exhibit smaller average interparticle spacings. For the unstretched sample, the Δ_{NMR} value is equal to the Δ_{TEM_ave} value, which reflects the more symmetric IPS distribution for this sample compared to the stretched samples (cf. Fig. 2c). In short, the NMR-based approach provides interparticle spacings that reflect the overall quality or homogeneity of clay dispersion in bulk materials.

In summary, an analytical relation was developed between NMR magnetization growth and interparticle spacings (IPS) of lamellar nanoparticulate relaxation sinks in polymeric nanocomposites. The approach is based on spin-diffusion-averaged paramagnetic enhanced ^1H NMR relaxometry, and was demonstrated on some montmorillonite-containing polypropylene nanocomposites. Interparticle spacings were determined from fitting the analytical relation to NMR relaxation data, and were found to agree with interparticle spacings determined by statistical analysis of TEM images. The NMR-derived spacings were consistent with TEM-measured quadratic mean IPS values when the IPS distribution was log-normal, and with TEM-measured arithmetic average IPS values when the IPS distribution was more random. Compared to the TEM data, the NMR-derived IPS values were found to reflect the overall quality, or homogeneity, of clay dispersion in the bulk material. These results provide new insights into the relationship between NMR relaxation and nanostructures in polymer matrices. While the focus here was lamellar nanoparticles in polymers, we believe that our NMR approach can be extended to characterize other nanomaterial fillers that fulfill the requisite assumptions. For rod-like or sphere-like particles, if their surface nuclei exhibit sufficiently fast relaxation (*e.g.*, $T_{1,s} \ll T_{1,m}$), their magnetization growth profiles should be described by a two- or three-dimensional model, simply expressed as the product of our 1D profile along two or three orthogonal directions.

Notes and references

1 Q. Wang, J. L. Mynar, M. Yoshida, E. Lee, M. Lee, K. Okuro, K. Kinbara, T. Aida, *Nature* 2010, **463**, 339-343.
2 C. Aulin, G. Salazar-Alvarez, T. Lindström, *Nanoscale* 2012, **4**, 6622-6628.
3 V. Nicolosi, M. Chhowalla, M. G. Kanatzidis, M. S. Strano, J. N. Coleman, *Science* 2013, **340**, 1226419.
4 G. Keledi, J. Hári, B. Pukánszky, *Nanoscale* 2012, **4**, 1919-1938.
5 B. Chen, J. R. G. Evans, H. C. Greenwell, P. Boulet, P. V. Coveney, A. A. Bowden, A. Whiting, *Chem. Soc. Rev.* 2008, **37**, 568-594.
6 X. Zhang, L. S. Loo, *Macromolecules* 2009, **42**, 5196–5207.
7 S. M. Liff, N. Kumar, G. H. McKinley, *Nature Mater.* 2007, **6**, 76–83.
8 T. Kashiwagi, F. M. Du, J. F. Douglas, K. I. Winey, R. H. Harris, J. R. Shields, *Nature Mater.* 2005, **4**, 928-933.
9 J. L. Suter, P. V. Coveney, *Soft Matter* 2009, **5**, 2239–2251.
10 P. Rittigstein, R. D. Priestley, L. J. Broadbelt, J. M. Torkelson, *Nature Mater.* 2007, **6**, 278-282.
11 T. D. Fornes, D. R. Paul, *Polymer* 2003, **44**, 4993-5013.
12 S. Salaniwal, S. K. Kumar, J. F. Douglas, *Phys. Rev. Lett.* 2002, **89**, 258301.
13 A. K. Kaushik, P. Podsiadlo, M. Qin, C. M. Shaw, A. M. Waas, A. N. Kotov, E. M. Arruda, *Macromolecules* 2009, **42**, 6588–6595.
14 B. Xu, Q. Zheng, Y. H. Song, Y. Shangguan, *Polymer* 2006, **47**, 2904-2910.
15 C. A. Diaz, Y. Xia, M. Rubino, R. Auras., *Nanoscale* 2013, **5**, 164–168.
16 J. M. Garces, D. J. Moll, J. Bicerano, R. Fibiger, D. G. McLeod, *Adv. Mater.* 2000, **12**, 1835-1839.
17 F. Hussain, M. Hojjati, M. Okamoto, R. E. Gorga, *J. Compos. Mater.* 2006, **40**, 1511-1575.
18 R. A. Vaia, in *Polymer-Clay Nanocomposites* (Eds.: T. J. Pinnavaia, G. W. Beal), John Wiley & Sons, New York, **2000**, pp. 229-266.
19 Z. P. Luo, J. H. Koo, *Polymer* 2008 **49**, 1841-1852.
20 Z. P. Luo, J. H. Koo, *J. Microscopy* 2007, **225**, 118-125.
21 B. Xu, J. Leisen, U. Boehme, U. Scheler, H. W. Beckham, *Z. Phys. Chem.* 2012, **226**, 1229-1241.
22 A. Jung, K. Peter, D. E. Demco, D. Jehnichen, M. Moeller, *Macromol. Chem. Phys.* 2012, **213**, 389-400.
23 M. Bertmer, M. F. Wang, M. Kruger, B. Blumich, V. M. Litvinov, M. van Es, *Chem. Mater.* 2007, **19**, 1089-1097.
24 C. Calberg, R. Jerome, J. Grandjean, *Langmuir* 2004, **20**, 2039-2041.
25 B. Xu, J. Leisen, H. W. Beckham, R. Abu-Zurayk, E. Harkin-Jones, T. McNally, *Macromolecules* 2009, **42**, 8959-8968.
26 D. L. VanderHart, A. Asano, J. W. Gilman, *Chem. Mater.* 2001, **13**, 3796-3809.
27 S. Bourbigot, D. L. VanderHart, J. W. Gilman, W. H. Awad, R. D. Davis, A. B. Morgan, C. A. Wilkie, *J. Polym. Sci. Part B: Polym. Phys.* 2003, **41**, 3188-3213.
28 A. Labouriau, Y. W. Kim, W. L. Earl, *Phys. Rev. B* 1996, **54**, 9952-9959.
29 A. Abragam, *The Principles of Nuclear Magnetism*, Clarendon Press, Oxford, **1961**.
30 P. G. de Gennes, *J. Phys. Chem. Solids* 1958, **7**, 345-350.
31 J. Clauss, K. Schmidt-Rohr, H. W. Spiess, *Acta Polym.* 1993, **44**, 1-17.
32 C. Hedesiu, D. E. Demco, R. Kleppinger, G. Vanden Poel, W. Gijsbers, B. Blumich, K. Remerie, V. M. Litvinov, *Macromolecules* 2007, **40**, 3977-3989.
33 D. W. Schaefer, R. S. Justice, *Macromolecules* 2007, **40**, 8501-8517.

^{a}School of Materials Science and Engineering, Georgia Institute of Technology, 801 Ferst Drive, Atlanta, GA 30332 USA.
^{b}School of Chemistry and Biochemistry, Georgia Institute of Technology, 901 Atlantic Drive, Atlanta, GA 30332 USA.
*E-mail: bxu6@gatech.edu

Nanoscale Accepted Manuscript

Journal Name

COMMUNICATION

[Type text]

Title

Nanoparticle Dispersion in Polymer Nanocomposites by Spin-Diffusion-Averaged Paramagnetic Enhanced NMR Relaxometry

Bo Xu,[a]* Johannes E. Leisen,[b] and Haskell W. Beckham[a]

The table of contents

An analytical relationship was developed that allows quantitative assessment of nanoparticle spacings in polymer/clay nanocomposites from NMR relaxometric data.

ToC Figure